



Comparison of whole exome sequencing in circulating tumor cells of primitive and metastatic nasopharyngeal carcinoma

Jinyuan Si^{1#}, Bo Huang^{2#}, Guiping Lan², Benjian Zhang², Jiazhang Wei², Zhuoxia Deng², Yiliang Li², Ying Qin², Bing Li², Yan Lu³, Yongfeng Si²

¹Department of Otolaryngology-Head and Neck Surgery, Xuanwu Hospital, Capital Medical University, Beijing, China; ²Department of Otolaryngology-Head and Neck Oncology, and Nasopharyngeal Carcinoma Institute, The People's Hospital of Guangxi Zhuang Autonomous Region, Nanning, China; ³SurExam Bio-Techs, Guangzhou Technology Innovation Base, Guangzhou, China

Contributions: (I) Conception and design: J Si; (II) Administrative support: Y Si; (III) Provision of study materials or patients: J Si, B Zhang, J Wei, Z Deng, Y Li, Y Qin, B Li, Y Lu; (IV) Collection and assembly of data: J Si, B Huang, G Lan, B Zhang; (V) Data analysis and interpretation: J Si, B Huang, G Lan, Y Si; (VI) Manuscript writing: All authors; (VII) Final approval of manuscript: All authors.

[#]These authors contributed equally to this work.

Correspondence to: Yongfeng Si, MD; Zhuoxia Deng. Department of Otolaryngology-Head and Neck Oncology, and Nasopharyngeal Carcinoma Institute, The People's Hospital of Guangxi Zhuang Autonomous Region, 6 Taoyuan Road, Nanning, China. Email: syfklxf@126.com; 13878858299@126.com.

Background: Nasopharyngeal carcinoma (NPC) is one of the most common cancers. To investigate the gene mutation profile of NPC patients, we performed whole exome sequencing (WES) in tumor cells, peripheral blood cells, and circulating tumor cells (CTCs) of primitive and metastatic NPC patients, and explored its clinical significance.

Methods: Primitive tumor cells, white blood cells, and CTCs of patients were collected and hybridized with probes targeting whole exons. Mutational signatures, signaling pathways, and cancer associated genes from CTCs cells of two primitive and two metastatic patients were analyzed using gene ontology (GO) method.

Results: The mutational landscape of four primitive tumors showed that there were more *MSH2* alterations in more non-silent mutation number patients. Additionally, *BAP1* gene mutation only occurred in metastatic patients. The most frequently mutated genes among the primitive tumor and CTC samples were *CEAP74*, *MOB3C*, *PDE4DIP*, *IGFN1*, *CYFIP2*, *NOP16*, *SLC22A1*, *ZNF117*, and *SSPO*. Interestingly, only *PMS1*, *BRIP1*, *DEE*, *OR2T12*, *CPN2*, *MLXIPL*, *BALAP3*, *IGSF3*, *SIN3B*, and *ZNF880* alterations occurred in primary tumors of metastatic patients. Primitive and metastatic NPC had significantly distinct mutational signatures. GO analysis revealed that each patient had his own mutational signaling pathways. Non-silent single nucleotide variations (non-silent SNVs) and insertion-deletion mutations (INDELs) in CTCs were more dramatic than in primitive tumor cells.

Conclusions: These changes are strongly relevant to their clinical characteristics and therapeutic strategy.

Keywords: Nasopharyngeal carcinoma (NPC); whole exome sequencing (WES); mutational signature; metastasis; circulating tumor cells (CTCs)

Submitted Dec 20, 2019. Accepted for publication Jun 03, 2020.

doi: 10.21037/tcr-19-2899

View this article at: <http://dx.doi.org/10.21037/tcr-19-2899>

Introduction

Nasopharyngeal carcinoma (NPC) is one of the most common cancers in humans and frequently has a history of

Epstein-Barr virus (EBV) infection associated with it and is prone to metastasize to distant lymph nodes and organs (1). The occurrence of NPC is a complex process that involves a combination of viral infection, environmental factors, and

genetic aberrations (2,3). It is also related to diet habits, including the consumption of salted fish (4). In addition, recent studies have revealed that alterations of *NF-κB* signal pathway genes are also strongly associated with the pathology of NPC (5-7). The treatment of NPC patients currently consists of combination of radiotherapy and chemotherapy, including the use of cisplatin, 5-fluorouracil (5-FU), paclitaxel, and gemcitabine (7-9). However, the prognosis of most NPC patients is still poor. Therefore, applying genetic screening to detect specific biomarkers for treatment may be a better option, especially for patients with metastasis. To date, some reports have shown that soluble programmed death-ligand1 (sPD-L1) (10-12), microRNAs BART7-3p, BART13-3p (13,14), amyloid beta 4 (A4) (15), and soluble MHC class I chain-related molecule A (MICA) (16) are good candidates as NPC biomarkers. However, the sensitivity and specificity of these biomarkers are controversial. Therefore, many studies have tried to explore new specific methods for NPC diagnosis and outcome predictions, including the clinical significance of circulating tumor cells (CTCs) in NPC patients (17,18). To date, less NPC genomic data are available, which obstructs the understanding of NPC biology, disease progression, and selective treatment.

Next generation sequencing (NGS) is a very sensitive and reliable technique for disclosing complex genetic aberrations in cancer patients (19). Chow *et al.* (8) found that there is a high percentage of gene mutations in fresh NPC samples, including alterations in the *EGFR-PI3K-Akt-mTOR*, *Notch*, *NF-κB*, and DNA damage and repair (DDR) signaling pathways. Lin *et al.* (20) reported that frequent genetic lesions in NPC patients were closely associated with chromatin modification, autophagy, and the *ERRBB-PI3K* signaling pathway. These reports mainly utilized primitive tumor cells as sequencing sources, which may have limited their outcomes. Recent studies have indicated that whole exome sequencing (WES) from patient's CTC samples reflect more accurately the genomic characterization of real tumors (21-23).

Here, we compared the gene mutations profiles of tumor cells and CTCs in primitive and metastatic NPC patients. CTCs originate from primitive tumors, where they are shed into the vasculature and/or lymphatics traveling in the blood circulation (24) to distant organs causing tumor metastasis. Therefore, the detection of CTC's genomic DNA alterations is very helpful to determine patient prognosis and the appropriate treatment.

Methods

Subjects

We collected and sequenced a total of 12 samples from four patients from June, 2017 to June, 2018 at our hospital. Their identification numbers were K06275, 47 year-old male; K06269, 54 year-old male; K05734, 62 year-old male; K06262, 54 year-old male. K06275 and K06269 were patients with non-metastatic NPC. K06262 and K05734 were patients with metastasis. Samples were taken from peripheral white blood cells, primitive tumors using surgery or endoscopy, and CTCs. This study protocol was conducted in accordance with the Declaration of Helsinki (as revised in 2013) and approved by ethical committee of the People's Hospital of Guangxi Zhuang Autonomous Region. Approved protocol number was 2017-23. All patients gave informed consent.

Samples DNA Extraction and CTCs isolation

DNA from the primitive lesions in paraffin embedded tumors was extracted using the Maxwell16 FFPE plus LEV DNA purification Kit (Promega, Madison, USA). For CTC isolation, we followed the protocols described as the previous paper (25). Briefly, 5 mL peripheral blood from the patient's vein was first lysed using red blood lysis buffer and then filtered through an 8 μm filter membrane. CTCs remained on the filter membrane, whereas white blood cells passed through the filter, after which, their DNA was extracted using the Maxwell 16 cell LEV DNA Purification kit (Promega, Madison, USA). The membrane with CTCs was hybridized using CanPatrol™ CTC RNAISH (SurExam Bio-Tech, Guangzhou, China) and identified. Then, confirmed CTCs were collected using a Palm Microbeam laser microdissection system and further enriched and amplified with the GenomePlex Single Cell. CTCs were classified as epithelial, mesenchymal, and mixed types according to their morphology and surface markers. Their graphs were shown as *Figure 1*. Whole Genome Amplification Kit (Sigma, USA). Finally, DNA fragments were obtained from amplify and purification and were used for all subsequent experiments.

DNA library generation and sequencing

The above mentioned DNA was processed for amplification of targeting regions, primers digestion, adapter connection,

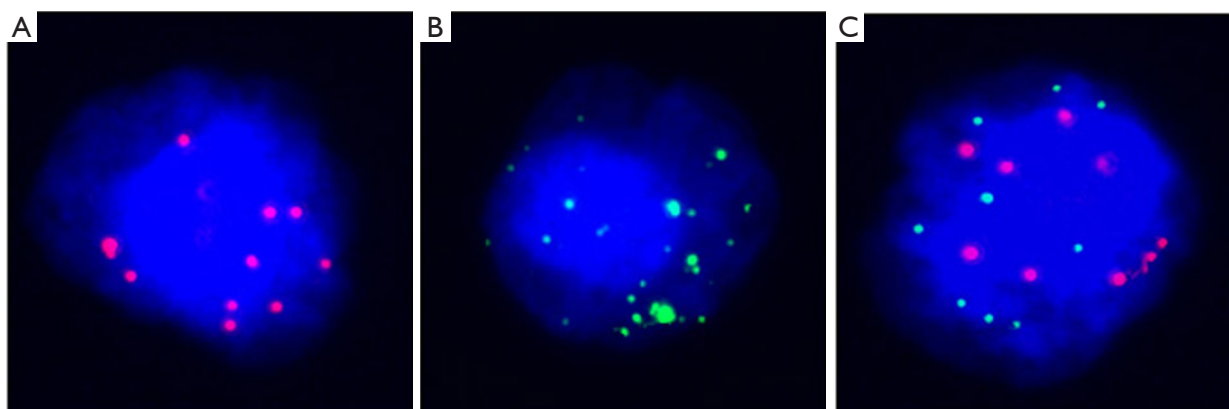


Figure 1 The graphs of circulating tumor cells (CTCs): (A) epithelial type CTCs, which detected by Alexa Fluor 594 (red color) labeled EpCAM,CK8, CK18,and CK19; (B) mesenchymal type CTCs, which detected by Alexa Fluor 488 labeled vimentin and Twist; (C) mixed CTCs were tested with epithelial and mesenchymal markers.

fragment screening, and library enrichment with the Ion AmpliSeq™ Exome RDY 4×2 kit (Life Technologies, USA). Then, a library was constructed, preparing sequencing template with the use of Ion Chef™ (Life Technologies, USA). The sequencing templates were then transferred into PI sequencing chips and connected to an Ion Proton sequencing instrument (Life Technologies, USA) for high-throughput sequencing (HTS).

Experiment flowchart

The exome is the sum of all exons in one specimen. This region contains essential genetic information for protein translation (26). Exome sequencing utilized chips and probes hybridizing genomic deoxyribonucleic acid (DNA) sequencing of riched exons. Then, high throughout sequencing was-used to detect all samples.

Bioinformatics analysis strategy

Raw reads were obtained from WES. Then, low quality (<10) sequences of less than 50 base pair were ruled out. After decontamination unique pairs were aligned with unique mapped reads in the whole genomic database. Subsequent genetic information analysis included targeting region sequencing depth, covering rate analysis, single-nucleotide polymorphism (SNP), and Indel detection, using the bioinformatics analysis tool Annovar. After screening for mutated genes with altered amino acid, we analyzed the linkage of the molecular mechanism, signal pathways and cellular functions in these altered genes and proteins using gene ontology (GO) analysis.

Results

Somatic mutational landscape in 4 NPC patients

To compare the profile of gene mutations in primitive and metastatic NPC patients, WES of white blood cells, tumor cells and CTCs from patients was performed and analyzed. All 4 patients were male. The age was between 47 to 62 years old. After ion torrent analysis of raw data of sequencing, they were screened and filtered. Then, we carried out Annovar analysis. Non-exonic region mutation sites, adapter, non-monoclonal fragments (multiple barcode), and synonymous mutations (SNV) were first ruled out. We chose non-synonymous mutations (non-SNV) as our data for analysis. The one of following three criteria was selected as our potential candidate genes: (I) significantly mutated genes previously reported in a large scale sequencing of NPC patients (20); (II) relevant genes in NPC as well as other cancers listed in the COSMIC database (<http://cancer.sanger.ac.uk/cosmic/>) (27); (III) genes that act in-pathways related to cancer according to the KEGG database (<https://www.genome.jp/kegg>). According to these criteria, we obtained the mutational landscape of 4 primitive tumor lesions (*Figure 2*). We found no significant difference between the non-SNV of the primitive lesions in the metastatic patients (K06262 and K05734) and the non-metastatic patients (K06269 and K06275). However, we found that there was *MSH2* gene mutation in two non-SNV patients (K06275 and K06262), which suggested that the *MSH2* gene mutation give rise to defects of the DDR function. This process in turn may have promoted the accumulation of mutations involved in tumorigenesis. In

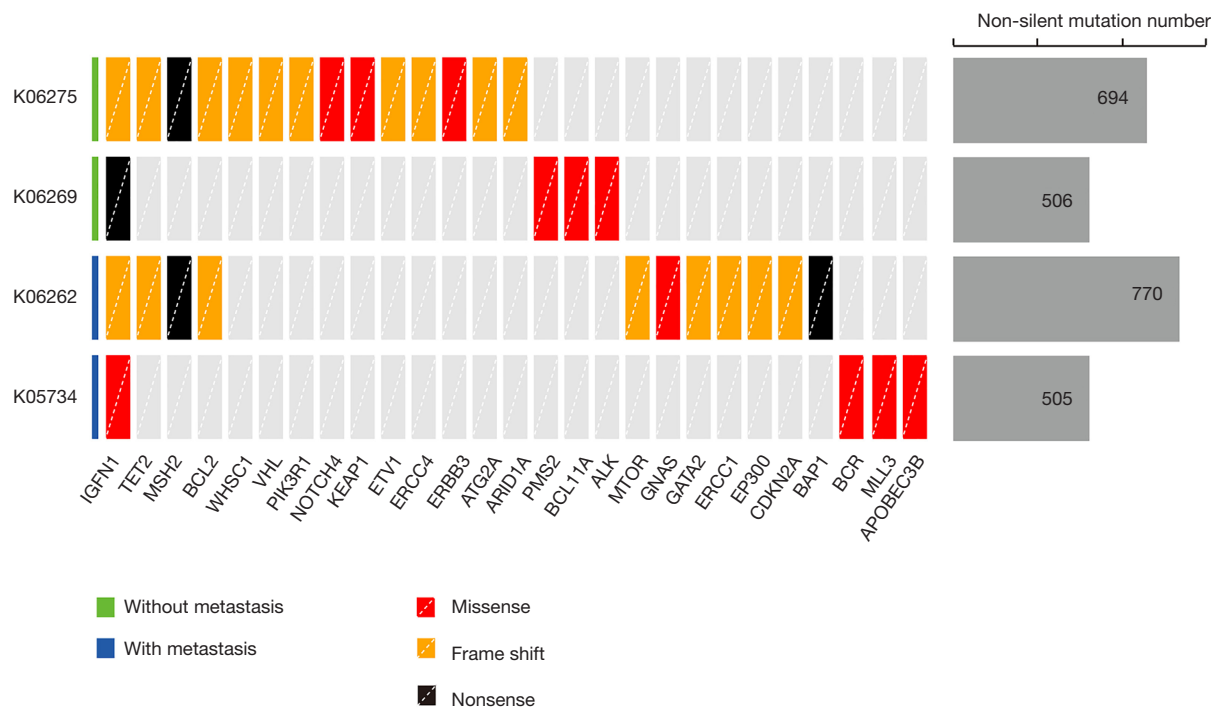


Figure 2 Mutational landscape of 4 nasopharyngeal carcinoma (NPC) primitive lesions: the left panel shows presence or absence of metastasis in the different patients; the middle panel shows driving mutations for each primitive tumor; the right panel shows non-silent mutation numbers (Non-SNV).

addition, we also found *BAP1* gene alteration in a metastatic patient (K06262), which is relevant to invasion and tumor metastasis (28). This result indicated that this gene mutation enhanced the invasive ability of cancer cells, and resulting in metastasis.

Mutational signature of the primary lesions and CTC samples

All single-nucleotide variations (SNVs) were classified into six categories according to the mutation directions (C > A, C > G, C > T, T > A, T > C, and T > G) (6). On the addition of mutated nucleotides at the 5'-terminal and 3'-terminal, there was total of 96 mutational contexts. Different mutational contexts have varying proportions in each tumor. This different ratio of 96 mutational contexts is defined as the mutational signature (29). Each signature has its corresponding generation mechanism. Therefore, we speculated that the mutational signature of each tumor contributes to its tumorigenesis. We analyzed a fraction of the 96 mutational contexts in four primitive NPC patients using the multiple linear regression models (30), and

compared their mutational contexts with 30 mutational signatures in the COSMIC database (*Figure 3*). The left panel in *Figure 3* shows a fraction of six mutational contexts and the right panel shows the proportion of each signature. We found that all the four patients had a dominant 3 type signature, which results from double strand DNA break and causes dysfunction of homologous recombination. This also indicated that the genome is unstable in the process of carcinogenesis. Interestingly, we also found the unique signatures 5 and 4 in two metastatic patients, K06262 and K05734, respectively. The resulting mechanism of signature 5 is unclear; however, it has been identified in many kinds of cancers. In contrast, signature4 frequently occurs as a C > A transition in the transcribed strand that results from smoking. These results indicated that distinct life environments and styles caused different carcinogenesis mechanisms.

To evaluate specific gene mutations in CTCs, we also performed differential mutation analysis. Gene mutations from leukocytes were used as a negative control. We found almost identical mutations between primitive tumor and white blood cells. In contrast, there were tremendous



Figure 3 Mutational signature framework of four primitive tumor samples. The left panel shows a fraction of mutational contexts in each patient. The right panel indicates mutational signature patterns.

differences between CTCs and white blood cells (Table 1). Specially, we found that *CFAP74*, *MOB3C*, *PDE4DIP*, *IGFN1*, *CYFIP2*, *NOP16*, *SLC22A1*, *ZNF117* and *SSPO* mutations were involved in both primary tumor and CTC samples. *CCDC144NL* only occurred in primitive tumors. Interestingly, *OR2T12*, *CPN2*, *MLXIPL*, *BALAP3*, *IGSF3*, *SIN3B*, and *ZNF880* mutations were found in the metastatic group (supplementary material at <http://fp.amegroups.cn/cms/123ade0661df777fed15ae4e1cea7fa/TCR-19-2899-1.xlsx>).

GO pathway enrichment analysis

We further analyzed the pathway enrichment of gene mutations using GO analysis. The results are shown in the Figures 4 and 5 for the NPC patients. As an example, the graph shows that the *UBC* complex, *ZNF* family numbers, *PCDH* proteins, and *IFNA* were key mutated genes in patient K06269 patient (Figure 4). In contrast, *PCDHGA10*, *SRA1*, *ZNF* family numbers, *CNOT1* and *WNK1* gene mutations were involved in alterations of signaling pathways

Table 1 Gene mutations in patient primary tumor (P_T) and circulating tumor cells (CTC)

Gene	K06269 P _T	K06275 P _T	K06262 P _T	K05734 P _T	K06269 CTC	K06275 CTC	K06262 CTC	K05734 CTC
<i>SAMD11</i>								cT257A
<i>NOC2L</i>					cT1532C, cG1531A, cA1529G, T672G		C2018_2020del, C1178_1179GA, cA92G	cA1024T, cG451A, c109_110del, cG67A
<i>KLHL17</i>					cA13G, G52A, cG1396A, cC1654A, cG1737C, cG1812A	cT1261C	cG1730C	cG1703A
<i>PLEKHN1</i>						cC1186T		cG568A, cA868G, cA1241G
<i>PERM1</i>					cA2299G, cT2204C, cA1652C, cC1649T, cG1640C, cG1626T, cT1105C, cA1096G, cT1085C, CT58A			cG1357A, cC713T, cC707T, cC457T
<i>ISG15</i>						cA188G		cG40A
<i>AGRN</i>					cG2404A, cC2423T, cC4688T, cA4696G, cA4697C, cG4924A, cG5883C	cG5536T, cG5626T	cT1732C, cA2066T, cG3421T, cG3433A, cG4324A, cG4456A	cT281C, cG1853A, cG2486A, cG2563A, cA2573G, cT2761C, cG4501A
<i>TTL10</i>					cC969A			c731delC, cG740A
<i>TNFRSF18</i>						cC562T		cC445T
<i>TNFRSF4</i>						cT446C		cG269A
<i>SDF4</i>					cG1015A, cG973A, cG763C, cG704A, cG657C, cG583A, cG280T, cG263A, cC259A, cC169A, cT143C			cC1022T, cC650T
<i>UBE2J2</i>					cT247C		cT239G	cT122C
<i>SCNN1D</i>							cG163C	cG587A, cA1978G
<i>ACAP3</i>					cG2204T, cG1789A, cG1733T, cG1637A, cT1616A, cG1475T, cA1474G, cG1468C, cG1432A			cC982T

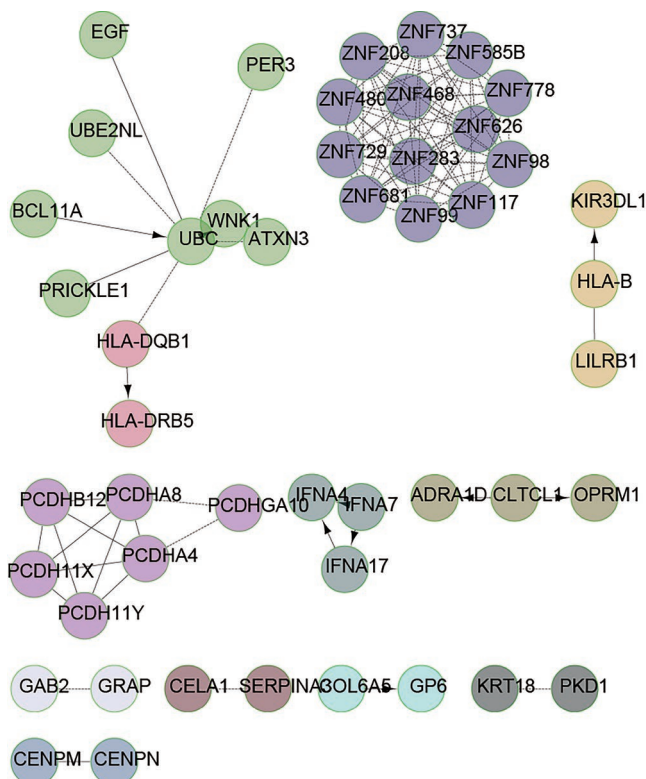


Figure 4 Pathway diagram summarizing the mutated genes in patient K06269. The results show that *UBC* complex, *ZNF* family numbers, *PCDH* proteins and *IFNA* are key mutated genes in K06269 patient.

in patient K05734 (Figure 5). Similarly, *HSPG2*, *NOTCH 4*, *PXN*, *PIK3R1* and *GAB1* gene mutations occurred in patient K06275. *CD40*, *HSPG2*, *EP300*, *LIMK1* and *GNAS* gene alteration were relevant to different signaling pathways in patient K06262 (data not shown). These data revealed that individual tumors had their own altered signaling pathways.

Profiles of cancer associated gene mutations

Carcinogenesis is a multi-step procession many gene mutations accumulate at various stages. Up to 400 genes including oncogenes, tumor suppressor, cell cycle related, apoptotic, RNA transcription and translation, DDR genes are involved in this transformation. The present study confirmed these findings in the metastatic patient K 06262 (Table 2). These critical gene mutations definitively contributed to the occurrence of NPC. We found *PMS2*, *BCL11A*, *PDE4DIP*, and *ALK4* gene mutations in the K06269 primitive lesion, which are related to DDR,

metabolism, cell proliferation, and protein degradation. In contrast, *ERCC3*, *EGFR*, *BRAF*, and 155 gene mutations occurred in K06269 CTC samples. Similarly, *MSH2*, *ERCC4*, *VHL*, and 21 more gene mutations occurred in the K06275 primary lesion; *PARP1*, *ERCC5*, *APC*, and 264 more gene mutations occurred in K06275 CTC samples. Interestingly, *MSH2*, *ERCC1*, *BAP1*, and 26 more gene mutations, and *MSH2*, *ERCC3*, *EGFR*, and 240 more gene mutations occurred in K06262 primitive lesion and CTC samples, respectively. *PDE4DI*, and *BCR2* mutations occurred in the patient K05734 primitive lesion. *MSH2*, *ERCC3*, *HIF1A*, and 237 more gene mutations occurred in the patient K05734 CTC sample (Table 3). We found that K06275 always had more mutations than the other three subjects in either primitive lesions or CTC samples. In contrast, subject K06262 from the metastatic group had more tumor associated gene mutations. Only K06262 had invasion relevant gene mutations in primitive lesions. However, all four CTC samples had more invasion and metastasis relevant gene mutations than primitive lesions.

Comparison of gene mutations in CTC samples

CTCs are considered one of the causes for cancer metastasis. Primitive tumor cells enter the peripheral blood and seed tumor cells into long distant organs, where they proliferate and amplify to form metastatic sites (31). We isolated CTCs from four patients using CTC isolation kits and performed WES to compare them with primitive tumors. The results are shown in Figure 6. We detected large amounts of somatic mutations. Although there were some identical mutations between primitive tumors and CTCs, we found that somatic mutations in CTCs were considerably higher than in the primitive tumor. These results indicated that CTC WES is very helpful tumor prediction and for diagnosis.

Discussion

Carcinogenesis is involved in the alteration of multiple molecules and signaling pathway networks (32,33). Activation of oncogenes or inactivation of suppressor genes can give rise to the occurrence of cancers (34,35). Here, we utilized WES to trace gene alterations in primitive tumors and CTCs of two non-metastatic patients and two metastatic patients. The present data revealed that the somatic mutation rate in CTCs is significantly higher than in either primitive tumor or metastatic samples.

Table 2 Function classification of gene mutations in K06262 primitive tumor sample

Gene	AACChange	ExonicFunc.refGene	Classification
<i>MSH2</i>	c.196_197insG	Stopgain	DNA damage and repair
<i>ERCC1</i>	c.211delG	Frameshift deletion	DNA damage and repair
<i>GATA2</i>	c.441dupG	Frameshift insertion	RNA transcription and translation
<i>TET2</i>	c.4582delC	Frameshift deletion	RNA transcription and translation
<i>PML</i>	c.1767delG	Frameshift deletion	RNA transcription and translation
<i>JAK3</i>	c.G2774T	SNV	RNA transcription and translation
<i>CRTC1</i>	c.1706delC	Frameshift deletion	RNA transcription and translation
<i>CEBPA</i>	c.206delC	Frameshift deletion	RNA transcription and translation
<i>CEBPA</i>	c.218_219del	Frameshift deletion	RNA transcription and translation
<i>CEBPA</i>	c.208_209del	Frameshift deletion	RNA transcription and translation
<i>CEBPA</i>	c.212delG	Frameshift deletion	RNA transcription and translation
<i>EP300</i>	c.4402dupA	Frameshift insertion	RNA transcription and translation
<i>PDE4DIP</i>	c.T5207A	SNV	Metabolism
<i>PDE4DIP</i>	c.C2353T	Stopgain	Metabolism
<i>PDE4DIP</i>	c.1218delA	Frameshift deletion	Metabolism
<i>PDE4DIP</i>	c.G180A	Stopgain	Metabolism
<i>RET</i>	c.960_961del	Frameshift deletion	Metabolism
<i>BCL9</i>	c.1148_1149insG	Frameshift insertion	Development and differentiation
<i>ACVR2A</i>	c.29_30insA	Frameshift insertion	Development and differentiation
<i>ACVR2A</i>	c.G31T	Stopgain	Development and differentiation
<i>TNK2</i>	c.21delC	Frameshift deletion	Development and differentiation
<i>HNF1A</i>	c.A1720G	SNV	Development and differentiation
<i>CIC</i>	c.407_408insC	Frameshift insertion	Development and differentiation
<i>IKBKB</i>	c.151delC	Frameshift deletion	Immunology
<i>CDKN2A</i>	c.342delC	Frameshift deletion	Apoptosis
<i>BCL2L2</i>	c.265delG	Frameshift deletion	Apoptosis
<i>EZH2</i>	c.1682delA	Frameshift deletion	Proliferation
<i>BCL2</i>	c.119_120del	Frameshift deletion	Proliferation
<i>TCF3</i>	c.1474delG	Frameshift deletion	Proliferation
<i>MARK4</i>	c.1310delG	Frameshift deletion	Proliferation
<i>MTOR</i>	c.3041_3042insT	Frameshift insertion	Signal transduction
<i>GNAS</i>	c.C1522A	SNV	Signal transduction
<i>BAP1</i>	c.G88T	Stopgain	Tumor metastasis

Table 3 Cancer associated gene mutations in primary tumor (PT) and CTC of NPC patients

Name	Classification	K06269 PT	K06275 PT	K06262 PT	K05734 PT	K06269 CTC	K06275 CTC	K06262 CTC	K05734 CTC
BRIP1	DNA damage						cT1904C	cC2443T, cA394C	
DEE	DNA damage							C795delA, C737del	
ERCC1	DNA damage		C211delG				cG [^] 10A		
ERCC2	DNA damage					cT1987C, cA1936C		cA523G	
ERCC3	DNA damage					cG421A, cA206G		cG163A	cC1611A
ERCC4	DNA damage		C1107delA					cG610A	
ERCC5	DNA damage					cA806G, cG2060A		cG1109A, c1232delC	cA1333C, cC2698T
FANCA	DNA damage					cA2069G, cT1171C		cT3322C	
FANCD2	DNA damage					cT328C, cC1382A		cA887T, cA2420G	cC221T, cT2245A
FANCG	DNA damage					cG248A, cT206C		cT866C, cG259A	cC1216T
MLH1	DNA damage					cT259A, cC671T	cA1138G		cG395A, cT578C
MRE11A	DNA damage						cT851C, cA517G	cT466C	
MSH2	DNA damage		C196-197invG	C196-197invG		cA37G, cT50C	cC1799T, cG1862A	cT2269A	cG847A, cT895C
MSH6	DNA damage					cG421C, cC587T	cA2367C, cT2959C		cG2689A, cA2822G
MUTYH	DNA damage					cA1583G, cT863C		cA155G	
NBN	DNA damage						cG1609G		cT2245C, c1181del
NSD1	DNA damage					cC73T, cA856C	cT3365C, cT4880C	cA527GcA1961C,	cT115C, cG634A
PALB2	DNA damage						cA2242T, cG829A	cT3215G, cT2593C	
PARP1	DNA damage					cA2108G, c1791delT	cA2173G, cT1982C	cG1480A, cG447C	cC2488A
PMS1	DNA damage					cC3017T, cG775C	cA133G, cA976G	C518delA	cG1390A, cT1652C
PMS2	DNA damage	cC1454A						cT866C	
RAD50	DNA damage					cG1131T, cA1192G	cC2354T, cA2930G	cA2567G, cT3664C	cA140G, c163delG
RECQL4	DNA damage						cG3552A, cT2282C	cC1415T	cT3083G, cC2309T

CTOs, circulating tumor cells; NPC, nasopharyngeal carcinoma.

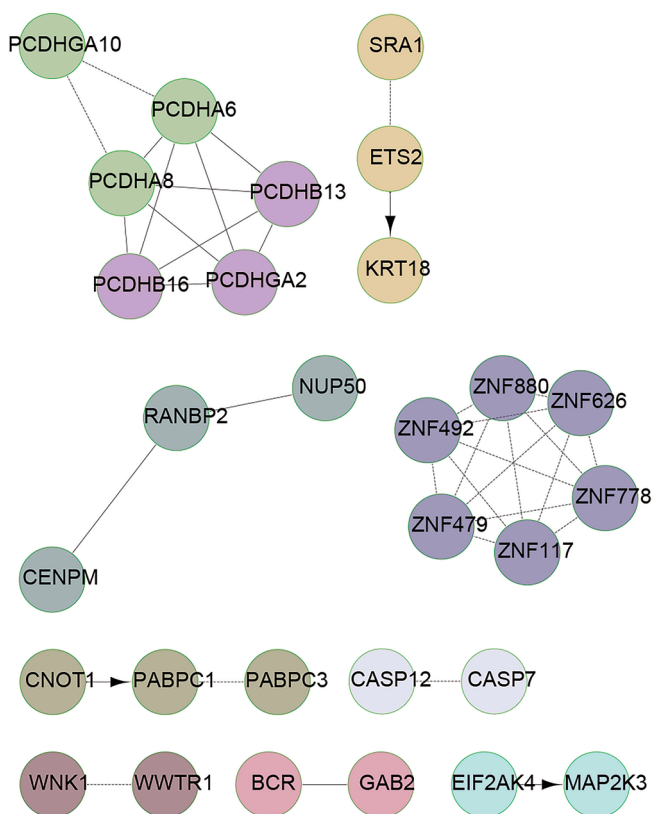


Figure 5 Pathway diagram summarizing the mutated genes in patient K05734. The graph shows that *PCDHGA10*, *SRA1*, *ZNF* family numbers, *CNOT1* and *WNK1* gene alterations are involved in the signaling pathways.

Interestingly, the patients with high non-synonymous mutations had *MSH2* gene mutation. In addition, we also found that *BAP1* gene alteration, which is relevant to invasion and metastasis of cancer, occurred in a metastatic patient.

MSH2 gene encodes a DNA mismatch repair (MMR) protein, which is involved in many kinds of DNA repair (36). *MSH2* alteration is frequently associated with hereditary nonpolyposis colorectal cancer (HNPCC) because of DNA microsatellite instability (37). Interestingly, immunotherapy of colorectal cancer patients with *MSH2* mutation has shown great benefits (38). Our qPCR results revealed that there were significant high PD-L1 and CTLA4 levels in metastatic patients compared with non-metastatic patients. Previous studies have shown extensive expression of PD-L1 had extensive expressions in tumor cells or immune cells of NPC patients (39,40). The other data also showed that there were high PD-L1 level in NPC patients with MMR

status (41). All together, these finding indicate that the use of immune checkpoint inhibitors in metastatic NPC patients may result in great outcomes. *MSH2* dimerizes with *MSH6* to form the MutS α mismatch repair complex, which repairs DNA longer insertion/deletion loops (42). *MSH2* alteration is also involved in acute lymphoblastoid leukemia (ALL) patients (43). Here, we found an association between *MSH2* mutations was associated in primitive and metastatic NPC patients with high somatic mutation ratio. This implied a key role of DDR gene dysfunction in the occurrence of NPC.

BAP1 gene encodes a deubiquitinating enzyme that acts as a nuclear-localizing protein. Mutations in this gene have been identified in some breast and lung cancers (27). *BAP1* mutation is closely relevant to metastasis (28). In the present result showed that *BAP1* alteration only happened in metastatic patient, confirming its role in metastasis. Two metastatic patients had the unique mutational signatures 4 and 5. This indicated that each patient is unique with his own environment and life style.

To date, previous reports have shown that sPD-L1 (10-12), microRNAs BART7-3p, BART13-3p (13,14), A4 (15), and MICA (16) as candidate biomarkers for NPC prognosis. The clinical significance of these markers for NPC metastasis remains. Recent studies revealed that gene mutations in the NF- κ B signaling pathway were involved in the occurrence of NPC (5,6,8,44). Our current data revealed that more gene mutation occurred in NPC patients, including those in DDR, RNA transcription and translation, metabolism, apoptosis, and immunology pathways. This result hinted that the occurrence of NPC is more complex than we previously thought. We also found that *CFAP74*, *MOB3C*, *PDE4DIP*, *IGFN1*, *CYFIP2*, *NOPI6*, *SLC22A1*, *ZNF117*, and *SSPO* mutations were present in all primitive tumor and CTC samples. Interestingly, *OR2T12*, *CPN2*, *MLXIPL*, *BAIAP*, *IGSF3*, *SIN3B* and *ZNF880* only occurred in metastatic NPC patients. This finding demonstrated that these genes may be used as new biomarkers to target therapy. We plan to test these mutated genes in large a sample size in the future.

We also found that many DDR relevant gene mutations including *BRIP1*, *PMS1* and *DEE* only existed in metastatic CTC samples. Graham *et al.* (45) found that *PMS1* forms a complex with *MIH1* gene to correct mispaired DNA. Zhao (46) reported that *MLH1*, *MSH2*, *MSH6* and *PMS1* are present in stage II and III colorectal cancer patients. Velázquez *et al.* (47) found that *BRIP1* gene mutations occurred in inherited breast cancer patients. It was also

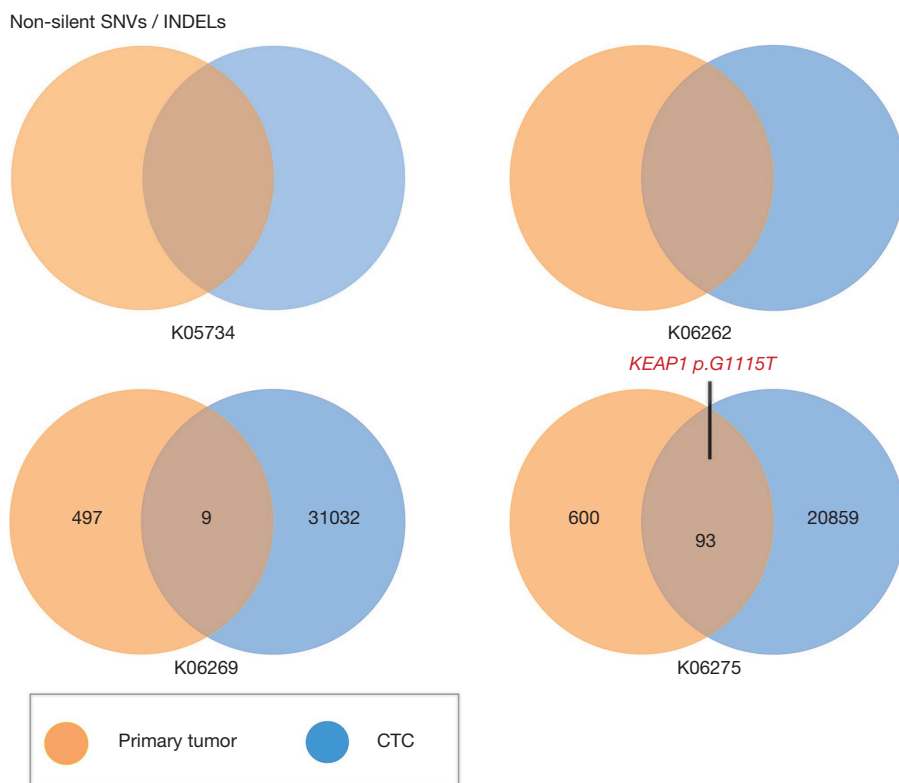


Figure 6 Comparison of cancer associated gene mutations in primitive tumors and CTCs. Venn diagram of the non-silent SNVs and INDELS in primitive lesion and CTC samples from 4 patients. SNVs, single nucleotide variations; INDELS, insertions and deletions.

reported that the association between *MSH6* and *BRIP1* variants are relevant to oxidative DNA damage in triple negative breast patients (48). Here, we first have found that *PMS1* and *BRIP1* gene mutations are relevant to NPC metastasis.

Conclusions

Our data revealed that WES of CTC samples in NPC patients is a very powerful tool for distinguishing primitive and metastatic tumor. We found that a few critical gene mutations, such as those in the *MSH2*, *BAP1*, *PMS1*, *DEE* and *BRIP1* genes are present in metastatic CTC samples. These genes may be used as new biomarkers to target treatment.

Acknowledgments

The authors would like to thank the support from the National Science Foundation of China and the Major Program of Science and Technology Development Project

of Guangxi Province.

Funding: This study was supported by the National Science Foundation of China (81760492) and by grants from the Major Program of Science and Technology Development Project of Guangxi Province (Grant no: GUIKEGONG 14124003-3).

Footnote

Data Sharing Statement: Available at <http://dx.doi.org/10.21037/tcr-19-2899>

Conflicts of Interest: All authors have completed the ICMJE uniform disclosure form (available at <http://dx.doi.org/10.21037/tcr-19-2899>). The authors have no conflicts of interest to declare.

Ethical Statement: The authors are accountable for all aspects of the work in ensuring that questions related to the accuracy or integrity of any part of the work are appropriately investigated and resolved. This study

protocol was conducted in accordance with the Declaration of Helsinki (as revised in 2013) and approved by ethical committee of the People's Hospital of Guangxi Zhuang Autonomous Region. Approved protocol number was 2017-23. All patients gave informed consent.

Open Access Statement: This is an Open Access article distributed in accordance with the Creative Commons Attribution-NonCommercial-NoDerivs 4.0 International License (CC BY-NC-ND 4.0), which permits the non-commercial replication and distribution of the article with the strict proviso that no changes or edits are made and the original work is properly cited (including links to both the formal publication through the relevant DOI and the license). See: <https://creativecommons.org/licenses/by-nc-nd/4.0/>.

References

1. Banko AV, Lazarevic IB, Folic MM, et al. Characterization of the Variability of Epstein-Barr Virus Genes in Nasopharyngeal Biopsies: Potential Predictors for Carcinoma Progression. *PLoS One* 2016;11:e0153498.
2. Zhang F, Zhang J. Clinical hereditary characteristics in nasopharyngeal carcinoma through Ye-Liang's family cluster. *Chin Med J (Engl)* 1999;112:185-7.
3. Lo KW, Chung GT, To KF. Deciphering the molecular genetic basis of NPC through molecular, cytogenetic, and epigenetic approaches. *Semin Cancer Biol* 2012;22:79-86.
4. Yu MC, Ho JH, Lai SH, et al. Cantonese-style salted fish as a cause of nasopharyngeal carcinoma: report of a case-control study in Hong Kong. *Cancer Res* 1986;46:956-61.
5. Li YY, Chung GT, Lui VW, et al. Exome and genome sequencing of nasopharynx cancer identifies NF-kappaB pathway activating mutations. *Nat Commun* 2017;8:14121.
6. Zheng H, Dai W, Cheung AK, et al. Whole-exome sequencing identifies multiple loss-of-function mutations of NF-kappaB pathway regulators in nasopharyngeal carcinoma. *Proc Natl Acad Sci U S A* 2016;113:11283-8.
7. Verhoeven RJ, Tong S, Zhang G, et al. NF-kappaB Signaling Regulates Expression of Epstein-Barr Virus BART MicroRNAs and Long Noncoding RNAs in Nasopharyngeal Carcinoma. *J Virol* 2016;90:6475-88.
8. Chow YP, Tan LP, Chai SJ, et al. Exome Sequencing Identifies Potentially Druggable Mutations in Nasopharyngeal Carcinoma. *Sci Rep* 2017;7:42980.
9. Bensouda Y, Kaikani W, Ahbeddou N, et al. Treatment for metastatic nasopharyngeal carcinoma. *Eur Ann Otorhinolaryngol Head Neck Dis* 2011;128:79-85.
10. Lu T, Chen Y, Li J, et al. High Soluble Programmed Death-Ligand 1 Predicts Poor Prognosis in Patients with Nasopharyngeal Carcinoma. *Onco Targets Ther* 2020;13:1757-65.
11. Wotman M, Herman SW, Costantino P, et al. The Prognostic Role of Programmed Death-Ligand 1 in Nasopharyngeal Carcinoma. *Laryngoscope* 2020. [Epub ahead of print].
12. Minichsdorfer C, Oberndorfer F, Krall C, et al. PD-L1 Expression on Tumor Cells Is Associated With a Poor Outcome in a Cohort of Caucasian Nasopharyngeal Carcinoma Patients. *Front Oncol* 2019;9:1334.
13. Lu T, Guo Q, Lin K, et al. Circulating Epstein-Barr virus microRNAs BART7-3p and BART13-3p as novel biomarkers in nasopharyngeal carcinoma. *Cancer Sci* 2020;111:1711-23.
14. Wu L, Wang J, Zhu D, et al. Circulating Epstein-Barr virus microRNA profile reveals novel biomarker for nasopharyngeal carcinoma diagnosis. *Cancer Biomark* 2020;27:365-75.
15. Li XY, Meng HL, Li KG, et al. Amyloid Beta (A4) Precursor Protein: A Potential Biomarker for Recurrent Nasopharyngeal Carcinoma. *Cancer Manag Res* 2019;11:10651-6.
16. Ben Chaaben A, Ouni N, Douik H, et al. Soluble MICA and anti-MICA Antibodies as Biomarkers of Nasopharyngeal Carcinoma Disease. *Immunol Invest* 2020;49:498-509.
17. Wen Z, Li Z, Yong P, et al. Detection and clinical significance of circulating tumor cells in patients with nasopharyngeal carcinoma. *Oncol Lett* 2019;18:2537-47.
18. Xie XQ, Luo Y, Ma XL, et al. Clinical significance of circulating tumor cells and their expression of cyclooxygenase-2 in patients with nasopharyngeal carcinoma. *Eur Rev Med Pharmacol Sci* 2019;23:6951-61.
19. Teng CF, Huang HY, Li TC, et al. A Next-Generation Sequencing-Based Platform for Quantitative Detection of Hepatitis B Virus Pre-S Mutants in Plasma of Hepatocellular Carcinoma Patients. *Sci Rep* 2018;8:14816.
20. Lin DC, Meng X, Hazawa M, et al. The genomic landscape of nasopharyngeal carcinoma. *Nat Genet* 2014;46:866-71.
21. Lohr JG, Adalsteinsson VA, Cibulskis K, et al. Whole-exome sequencing of circulating tumor cells provides a window into metastatic prostate cancer. *Nat Biotechnol* 2014;32:479-84.
22. Dai W, Zheng H, Cheung AK, et al. Whole-exome sequencing identifies MST1R as a genetic susceptibility gene in nasopharyngeal carcinoma. *Proc Natl Acad Sci U*

- S A 2016;113:3317-22.
23. Tyner JW, Tognon CE, Bottomly D, et al. Functional genomic landscape of acute myeloid leukaemia. *Nature* 2018;562:526-31.
 24. Riquet M, Rivera C, Gibault L, et al. Lymphatic spread of lung cancer: anatomical lymph node chains unchained in zones. *Rev Pneumol Clin* 2014;70:16-25.
 25. Wu S, Liu S, Liu Z, et al. Classification of circulating tumor cells by epithelial-mesenchymal transition markers. *PLoS One* 2015;10:e0123976.
 26. Gilbert W. Why genes in pieces? *Nature* 1978;271:501.
 27. Jensen DE, Proctor M, Marquis ST, et al. BAP1: a novel ubiquitin hydrolase which binds to the BRCA1 RING finger and enhances BRCA1-mediated cell growth suppression. *Oncogene* 1998;16:1097-112.
 28. Harbour JW, Onken MD, Roberson ED, et al. Frequent mutation of BAP1 in metastasizing uveal melanomas. *Science* 2010;330:1410-3.
 29. Alexandrov LB, Nik-Zainal S, Wedge DC, et al. Signatures of mutational processes in human cancer. *Nature* 2013;500:415-21.
 30. Rosenthal R, McGranahan N, Herrero J, et al. DeconstructSigs: delineating mutational processes in single tumors distinguishes DNA repair deficiencies and patterns of carcinoma evolution. *Genome Biol* 2016;17:31.
 31. Ni X, Zhuo M, Su Z, et al. Reproducible copy number variation patterns among single circulating tumor cells of lung cancer patients. *Proc Natl Acad Sci U S A* 2013;110:21083-8.
 32. Fearon ER, Vogelstein B. A genetic model for colorectal tumorigenesis. *Cell* 1990;61:759-67.
 33. Knudson AG. Two genetic hits (more or less) to cancer. *Nat Rev Cancer* 2001;1:157-62.
 34. Vlahopoulos SA, Logotheti S, Mikas D, et al. The role of ATF-2 in oncogenesis. *Bioessays* 2008;30:314-27.
 35. Matoba S, Kang JG, Patino WD, et al. p53 regulates mitochondrial respiration. *Science* 2006;312:1650-3.
 36. Pitsikas P, Lee D, Rainbow AJ. Reduced host cell reactivation of oxidative DNA damage in human cells deficient in the mismatch repair gene hMSH2. *Mutagenesis* 2007;22:235-43.
 37. Bonis PA, Trikalinos TA, Chung M, et al. Hereditary nonpolyposis colorectal cancer: diagnostic strategies and their implications. *Evid Rep Technol Assess (Full Rep)* 2007;(150):1-180.
 38. Overman MJ, Ernstoff MS, Morse MA. Where We Stand With Immunotherapy in Colorectal Cancer: Deficient Mismatch Repair, Proficient Mismatch Repair, and Toxicity Management. *Am Soc Clin Oncol Educ Book* 2018;38:239-47.
 39. Larbcharoensub N, Mahaprom K, Jiarpinitnun C, et al. Characterization of PD-L1 and PD-1 Expression and CD8+ Tumor-infiltrating Lymphocyte in Epstein-Barr Virus-associated Nasopharyngeal Carcinoma. *Am J Clin Oncol* 2018;41:1204-10.
 40. Chan OS, Kowanetz M, Ng WT, et al. Characterization of PD-L1 expression and immune cell infiltration in nasopharyngeal cancer. *Oral Oncol* 2017;67:52-60.
 41. Zhao L, Liao X, Hong G, et al. Mismatch repair status and high expression of PD-L1 in nasopharyngeal carcinoma. *Cancer Manag Res* 2019;11:1631-40.
 42. Downen JM, Putnam CD, Kolodner RD. Functional studies and homology modeling of Msh2-Msh3 predict that mismatch recognition involves DNA bending and strand separation. *Mol Cell Biol* 2010;30:3321-8.
 43. Diouf B, Cheng Q, Krynetskaia NF, et al. Somatic deletions of genes regulating MSH2 protein stability cause DNA mismatch repair deficiency and drug resistance in human leukemia cells. *Nat Med* 2011;17:1298-303.
 44. Li Y, Qin Y, Yang C, et al. Cardamonin induces ROS-mediated G2/M phase arrest and apoptosis through inhibition of NF-kappaB pathway in nasopharyngeal carcinoma. *Cell Death Dis* 2017;8:e3024.
 45. Graham WJ, Putnam CD, Kolodner RD. The properties of Msh2-Msh6 ATP binding mutants suggest a signal amplification mechanism in DNA mismatch repair. *J Biol Chem* 2018;293:18055-70.
 46. Zhao L. Mismatch repair protein expression in patients with stage II and III sporadic colorectal cancer. *Oncol Lett* 2018;15:8053-61.
 47. Velázquez C, Esteban-Cardenosa EM, Lastra E, et al. Unraveling the molecular effect of a rare missense mutation in BRIP1 associated with inherited breast cancer. *Mol Carcinog* 2019;58:156-60.
 48. Aravind Kumar M, Naushad SM, Narasingu N, et al. Whole exome sequencing of breast cancer (TNBC) cases from India: association of MSH6 and BRIP1 variants with TNBC risk and oxidative DNA damage. *Mol Biol Rep* 2018;45:1413-9.

Cite this article as: Si J, Huang B, Lan G, Zhang B, Wei J, Deng Z, Li Y, Qin Y, Li B, Lu Y, Si Y. Comparison of whole exome sequencing in circulating tumor cells of primitive and metastatic nasopharyngeal carcinoma. *Transl Cancer Res* 2020;9(7):4080-4092. doi: 10.21037/tcr-19-2899